

Side chain effects on photoinduced absorption and photovoltaic performance of low bandgap thienylene vinylene and phenylene vinylene copolymers

L.H. Nguyen^{1,a}, S. Günes¹, H. Neugebauer¹, N.S. Sariciftci¹, K. Colladet², S. Fourier², T.J. Cleij², L. Lutsen³, J. Gelan^{2,3}, and D. Vanderzande^{2,3}

¹ Linz Institute for Organic Solar Cells (LIOS), Johannes Kepler University, Altenbergerstr. 69, 4040 Linz, Austria

² Hasselt University, Institute for Materials Research (IMO), Agoralaan, Building D, 3590 Diepenbeek, Belgium

³ IMEC, Division IMOMECE, Wetenschapspark 1, 3590 Diepenbeek, Belgium

Received: 21 July 2006 / Accepted: 6 October 2006

Published online: 6 December 2006 – © EDP Sciences

Abstract. In this work low bandgap thienylenevinylene and phenylene vinylene copolymers, which possess either 3,4-ethylenedioxythiophene (EDOT) groups (Polymer 1) or long alkyl side chains (Polymer 2) were investigated and compared in photoinduced electron transfer properties and photovoltaic performance. The results show that the interaction of the photoexcited polymers with an electron acceptor ([6,6]-phenyl C61 – butyric acid methyl ester (PCBM)) leads to charge generation and transfer for both polymers. We found that the long alkyl side chain in Polymer 2 instead of the EDOT group in Polymer 1 enhances the open circuit voltage (V_{OC}) but lowers the short circuit current (I_{SC}). On the other hand the long alkyl side chain in Polymer 2 significantly improves the solubility and enhances processability for solar cells fabrication. Optimization of the chemical structure of these low bandgap polymers could lead to a spectral improvement of photocurrent generation in organic solar cells.

PACS. 85.60.-q Optoelectronic devices – 85.60.Bt Optoelectronic device characterization, design, and modeling – 85.60.Dw Photodiodes; phototransistors; photoresistors

1 Introduction

Organic photovoltaic devices are promising candidates as renewable source of electrical energy because of its ease in fabrication and low production cost as well as light weight and flexibility. The best reported devices are today able to achieve 2.5–5% power efficiency [1,2] employing the bulk heterojunction concept which ensures a large interfacial area for efficient charge generation. However, the demand for overcoming the mismatch of the absorption spectrum and the solar emission may continue to enhance the photovoltaic performance. Low bandgap conjugated polymers, which absorb at longer wavelengths, have appeared as a new approach and still remain the focus of strong interest for organic solar cells application because they may improve the efficiency compared to other traditional materials as polyphenylene-vinylenes and polythiophenes.

One of the most promising strategies to tailor the energy levels of conjugated polymers is the donor-acceptor route concept from which the interaction between alternating electron rich donors and electron deficient accep-

tors will result in a compressed band gap [3–5]. In this work we used conjugated polymers based on bis-(1-cyano-2-thienylvinylene)phenylene whose structure consists of a central dialkoxyphenylene core p-disubstituted by two thiophene derivatives through a cyanovinylene linker. We investigated and compared these two polymers which possess either EDOT (namely Polymer 1, *P1*) or long alkyl side chain C_8H_{17} on the thiophene part (namely Polymer 2, *P2*) towards photoinduced electron transfer and photovoltaic performance. A further decrease of the oxidation potential was obtained by the incorporation of the more electron rich EDOT (*P1*) while the long alkyl side chain on the thiophene part played the role of extra solubilizing chains [5]. The results show that the interaction of the photoexcited polymers with an electron acceptor ([6,6]-phenyl C61 – butyric acid methyl ester (PCBM)) leads to charge generation and transfer for both polymers. We found that the long alkyl side chain in *P2* instead of the EDOT group in *P1* enhances the open circuit voltage (V_{OC}) but lowers the short circuit current (I_{SC}). A correlation between the photophysical study, achievable solar cell performances and corresponding nanomorphologies is drawn in conclusion.

^a e-mail: lehuong.nguyen@jku.at; Lhnguyen@gmx.at

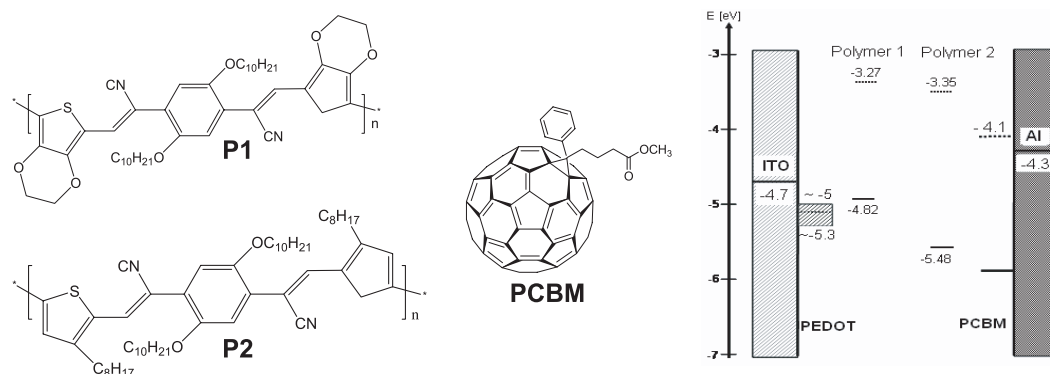


Fig. 1. Chemical structures (left) of Polymer 1 (*P1*), Polymer 2 (*P2*), PCBM and their energy levels (right).

2 Experimental section

2.1 Materials

The chemical structure of the low bandgap polymers *P1* ($M_w = 199\,000$, $M_n = 65\,000$, $DP = 2.9$), *P2* ($M_w = 35\,000$, $M_n = 15\,000$, $DP = 2.3$) [5] and [6,6]-phenyl C61 – butyric acid methyl ester (PCBM) with their energy levels [5] are shown in Figure 1.

2.2 Optical absorption

Thin film samples for optical measurements were prepared by spincoating from chloroform solution onto the glass substrates. The spectra were recorded using Varian Cary 3G UV-Vis Spectrophotometer.

2.3 Photomodulation spectroscopy

Photoinduced absorption (PIA) measurements were performed on the pristine and the blend films with 1:2 weight ratio of polymer/PCBM. The sample film was mounted in a cryostat (Oxford CF 204) and held at 80 K under vacuum better than 10^{-5} mbar. Photoinduced changes in the absorption spectra were recorded by mechanical chopping the pump beam of an argon laser (514 nm, 40 mW, INNOVA 400) at 218 Hz. The transmission T and the photoinduced changes ΔT in the spectral range of 600–2200 nm were measured using a detector and lock in amplifier technique. The photoluminescence (*PL*) spectra were recorded without probe beam on the sample using the same settings.

2.4 Atomic force microscopy (AFM)

AFM studies were performed by using a Digital Instruments Dimension 3100 in the tapping mode. The AFM characterization was performed in an area of the active layer of the photovoltaic device where the electrode was not deposited.

2.5 Solar cell fabrication

Using the bulk heterojunction concept, photovoltaic devices were fabricated from a blend of the polymer as a donor and PCBM as an acceptor. A solution of the polymer and PCBM in a 1:2 wt. was prepared in chloroform with a total concentration of 10 mg/ml. Poly(3,4-ethylenedioxythiophene):poly(styrenesulfonate) (PEDOT:PSS) (Baytron P) was spincoated on top of an indium-tin oxide (ITO) coated glass ($\sim 25 \Omega/\text{sq}$). Then the active layer (polymer:PCBM blend) was spincoated on the PEDOT:PSS layer (about 80 nm thick). 6 Å of lithium fluoride (LiF) and an 80 nm thick Al electrode was deposited on the blend film by thermal evaporation at $\sim 5 \times 10^{-6}$ mbar. Device annealing was carried out inside a glove box at 120 °C for 4 min. All current-voltage (*I-V*) characteristics of the photovoltaic devices were measured using a Keithley SMU 2400 unit under inert atmosphere (argon) in a dry glove box. A Steuernagel solar simulator under AM 1.5 conditions was used as the excitation source with an input power of 100 mWcm^{-2} white light illumination. A lock-in technique was used to measure the incident photon-to-current efficiency (IPCE).

3 Results and discussion

3.1 Photophysics

Figure 2 shows optical absorption (grey lines) and *PL* (black solid lines) of pristine *P1* and *P2*. The optical absorption spectrum of *P1* shows a maximum at about 650 nm with the onset of the $\pi - \pi^*$ transition at about 820 nm ($\sim 1.5 \text{ eV}$) (Fig. 2a), while *P2* exhibits a blue shift in the absorption with a maximum at 550 nm and the optical bandgap of about 1.8 eV (Fig. 2b). *PL* of the polymers (*P1* or *P2*) and their blend with PCBM was measured to check if there is an interaction of the two components in the excited state. *PL* quenching is often indicative of a charge transfer for many donor-acceptor blends [6]. *P2* shows stronger *PL* compared to *P1*. In both cases when adding PCBM as an acceptor at ratio 1:2 wt the intense *PL* of the pristine polymers is quenched by a factor of 4–5 (dashed lines in Figs. 2a, b for *PL* of the blends), implying

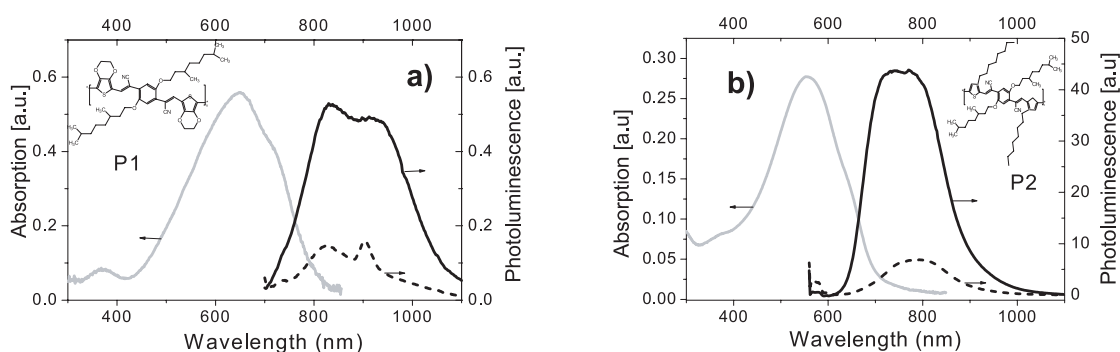


Fig. 2. Optical absorption and photoluminescence of pristine polymer and its blend with PCBM: (a) for *P1*; (b) for *P2*.

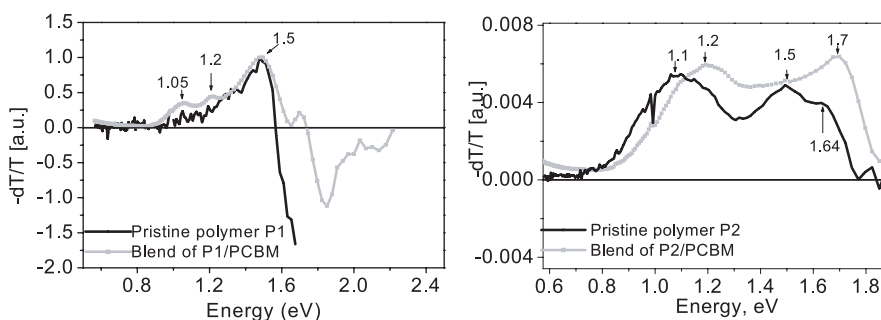


Fig. 3. PIA spectra of pristine polymer (black line) and polymer: PCBM at 1:2 wt. (grey line) recorded at 80 K following chopped cw excitation at 514 nm, 218 Hz: (a) for *P1*; (b) for *P2*.

that there is an interaction between the two components in the excited state.

The PIA spectra of pristine *P1* and a blend of *P1*:PCBM (1:2 wt) films are shown in Figure 3a. The PIA spectrum of the pristine *P1* exhibits a pronounced single absorption peak at 1.49 eV (black line), which is attributed to a $T_n \leftarrow T_1$ transition of the T_1 triplet excited state. In the mixture with PCBM three new peaks are observed at <0.8 eV, 1.05, 1.2, (grey line, Fig. 3a). We propose the weak PIA bands around <0.8 eV and 1.05 are attributed to low-energy (LE) and high-energy (HE) polaronic absorptions. A PIA band around 1.2 eV is assigned to the known absorption of the methanofullerene radical anion which was often observed at 1.15 to 1.2 eV [7,8]. The obtained PIA results supported by PL quenching indicate the evidence for charge transfer in the composite upon photoexcitation.

Two PIA features of pristine *P2* are observed at 1.1 and 1.49 eV with an additional shoulder at 1.64 eV (black line, Fig. 3b). The photoexcitation pattern of *P2* is more complicated compared to that of *P1*. This could be the results of the disorder effect introduced by the long alkyl side chain (C_8H_{17}) in *P2*. The PIA of the composite of *P2* with PCBM (1:2 wt) (grey line, Fig. 3b) shows analogous absorption features at 1.2 and 1.7 eV. Additionally observation of a weak absorption is obtained at <0.7 eV which is assigned for LE absorption. The broad absorption centered at 1.2 eV is proposed to the contribution of the overlapping between the shifted peak at 1.1 eV and the PCBM radical anion band (expected at 1.2 eV). Hence,

there is indication of photoinduced charge generation in this composite system. The occurrence of charge transfer is confirmed by the quenching of the PL by a factor of 5 when adding PCBM into the *P2* (Fig. 2b). Furthermore this evidence for charge transfer from *P2* to the PCBM in the blend is also well confirmed by light-induced electron paramagnetic resonance results [5].

3.2 Solar cells

Typical semilogarithmic *I-V* characteristics of ITO/PEDOT:PSS/*P1*:PCBM/LiF/Al (named *P1* device) and ITO/PEDOT:PSS/*P2*:PCBM/LiF/Al (named *P2* device) devices are shown, both in dark (dashed-dot lines) and under AM 1.5 illumination (solid lines), in Figure 4a. The *P2* (grey lines) device performance shows open circuit voltages (V_{OC}) of 650 mV, short circuit currents (I_{SC}) of $0.5 \text{ mA}\cdot\text{cm}^{-2}$, fill factors (FF) of 0.42 and the conversion efficiency (η) of about 0.14 % while the *P1* (black lines) device exhibits lower V_{OC} (400 mV), lower FF (0.22) but significantly higher I_{SC} ($1.64 \text{ mA}\cdot\text{cm}^{-2}$) leading to the same value of $\eta = 0.14\%$. Optimization of the device parameters by thermal annealing shows a slight increase in photovoltaic performance for the *P1* device with the following characteristics: $V_{OC} = 350$ mV, $I_{SC} = 1.87 \text{ mA}\cdot\text{cm}^{-2}$, $FF = 0.29$ (black lines in Fig. 4a) which results in $\eta = 0.19\%$ while annealing has not shown improvement effects for the *P2* device.

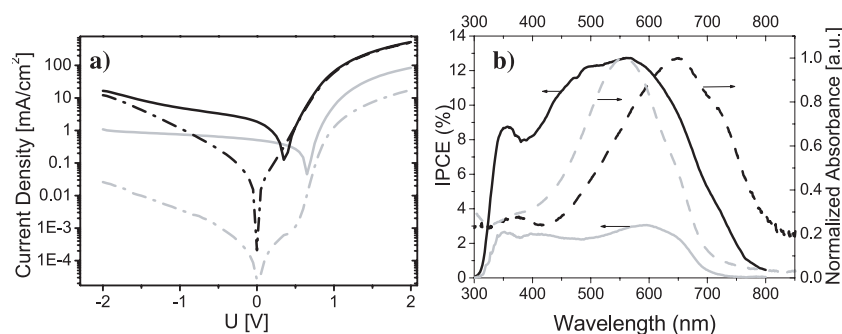


Fig. 4. (a) Semilogarithmic representations of I - V characteristics (AM 1.5, $100 \text{ mW}\cdot\text{cm}^{-2}$) of devices $P1$ (black lines) and device $P2$ (grey lines). The solid lines represent data obtained under illumination, while the dashed lines are measured in the dark. (b) Photocurrent spectrum IPCE (solid lines) of devices $P1$ (black line) and $P2$ (grey line) and the optical absorptions of the corresponding pristine polymers (dashed lines).

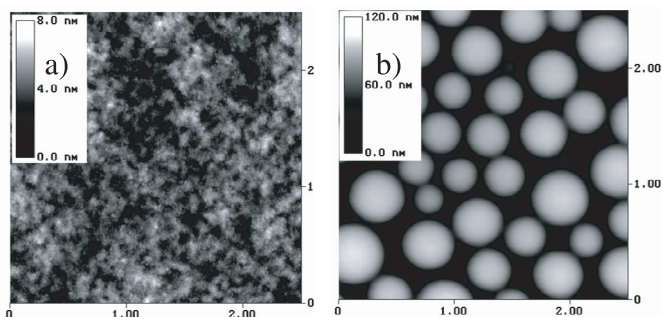


Fig. 5. AFM nanomorphology of $P1$ (a) and $P2$ (b) device films.

Figure 4b compares the spectrally resolved photocurrent (IPCE) of devices $P1$ (solid black line) and $P2$ (solid grey line) together with the corresponding absorption spectra of pristine polymers (dashed lines). The IPCE spectrum of the $P2$ device shows an onset at about 700 nm ($\sim 1.8 \text{ eV}$) close to the optical band gap and exhibits a maximum of 3% at 600 nm while the IPCE spectrum for $P1$ device extends its onset to higher wavelength at about 780 nm ($\sim 1.6 \text{ eV}$) with a maximum absorption of more than 12% at 550 nm. $P1$ possesses a quite low band gap ($E_g \sim 1.5 \text{ eV}$) resulting in an increase in absorption of light. As a consequence the I_{SC} increases but at the same time V_{OC} is lowered because the V_{OC} of polymer/fullerene-based solar cells depends on the energy difference between the HOMO of the donor and the LUMO of the acceptor [9]. The octyl substitution in $P2$ decreases the oxidation potentials as compared with the non-substituted analogue as a result of the increased electron donating effect by the octyl chain [5]. This leads to an increase in V_{OC} for $P2$ device.

To gain more insight into the effects of alkyl side chains on photoinduced charge transfer and photovoltaic performance, the morphology of the active layers was investigated. Figure 5 shows the nanomorphology of the active layers of $P1$ and $P2$ devices. Going from $P1$ to $P2$ with the introduction of the long alkyl side chains the surface roughness is increased which points directly to an in-

creased nanoscale phase-separation within the blend film. Both polymer structures consist of the long alkoxychains on the central core to provide the solubility of the polymers. A $P1$ device film shows a flat surface, no significant phase separation while dramatically larger phase separation was observed in the case of $P2$ which may point to an alkyl side chain effect. Consequently the interfacial area in the active layer $P2$ blend is reduced (compared to $P1$) leading to insufficient charge generation and separation in the $P2$ blend. As a result I_{SC} of $P2$ device is reduced significantly. We note that the morphology can be influenced by other parameters as different solvents, etc. However in this case, the large phase separation obtained for $P2$ appears rather as an issue of the alkyl side chain effect than as a solubility problem because the introduction of extra solubilizing chains for $P2$ on thiophene unit additionally increases the solubility of the $P2$ [5].

4 Conclusions

In summary, signatures of photoinduced charge generation were found in the systems of the bis-(1-cyano-2-thienylvinylene)phenylene based polymers ($P1$ and $P2$) with PCBM. However, for practical applications, the charge transfer seems not to be strongly efficient in these systems. A cross-relation between the achievable solar cell performance and the corresponding nanomorphology interlinked to the photophysics is concluded. Both polymers exhibit low band gap and show spectral improvements of photocurrent generation in organic solar cells. Obviously, the long alkyl side chain instead of EDOT group enhanced the V_{OC} but lower the I_{SC} . The long alkyl side chain with disorder effect may reduce the hole mobilities which result in low short circuit currents.

This work was performed as a part of the European Union funded research, project MOLYCELL (project No. SES6-CT-2003-502783). We would like to acknowledge the financial support from MOLYCELL project.

References

1. S.E. Shaheen, C.J. Brabec, N.S. Sariciftci, F. Padinger, T. Fromherz, J.C. Hummelen, *Appl. Phys. Lett.* **78**, 841 (2001)
2. W. Ma, C. Yang, X. Ong, K. Lee, A.J. Heeger, *Adv. Funct. Mater.* **15**, 1617 (2005)
3. H.A.M. van Mullekom, J. Vekemans, E.E. Havinga, E.W. Meijer, *Mat. Sci. Eng. R* **32**, 1 (2001)
4. K. Colladet, M. Nicolas, L. Goris, L. Lutsen, D. Vanderzander, *Thin Solid Films* **451**, **452**, 7 (2004)
5. K. Colladet, S. Fourier, T.J. Cleij, L. Lutsen, J. Gelan, D. Vanderzande, L.H. Nguyen, H. Neugebauer, N.S. Sariciftci, *Low Band Gap Donor-Acceptor Conjugated Polymers towards Organic Solar Cells Applications* (accepted by *Macromolecules*)
6. N.S. Sariciftci, L. Smilowitz, A.J. Heeger, F. Wudl, *Science* **258**, 1474 (1992)
7. L. Smilowitz, N.S. Sariciftci, R. Wu, C. Gettinger, A.J. Heeger, F. Wudl, *Phys. Rev. B* **47**, 13835 (1993)
8. K. Lee, E.K. Miller, N.S. Sariciftci, J.C. Hummelen, F. Wudl, A.J. Heeger, *Phys. Rev. B* **54**, 10525 (1996)
9. C.J. Brabec, N.S. Sariciftci, J.C. Hummelen, *Adv. Funct. Mater.* **11**, 15 (2001)